MOLECULAR AND CELLULAR BIOLOGY, July 2007, p. 5172–5183 Vol. 27, No. 14
0270-7306/07/$08.00+0 doi:10.1128/MCB.02298-06

Myosin 5a Is an Insulin-Stimulated Akt2 (Protein Kinase Bβ) Substrate Modulating GLUT4 Vesicle Translocation▽

Takeshi Yoshizaki, Takeshi Imamura, Jennie L. Babendure, Juu-Chin Lu, Noriyuki Sonoda, and Jerrold M. Olefsky*

Division of Endocrinology and Metabolism, Department of Medicine, University of California, San Diego, 9500 Gilman Dr., La Jolla, California 92093

Received 8 December 2006/Returned for modification 31 January 2007/Accepted 7 May 2007

Phosphatidylinositol 3-kinase activation of Akt signaling is critical to insulin-stimulated glucose transport and GLUT4 translocation. However, the downstream signaling events following Akt activation which mediate glucose transport stimulation remain relatively unknown. Here we identify an Akt consensus phosphorylation motif in the actin-based motor protein myosin 5a and show that insulin stimulation leads to phosphorylation of myosin 5a at serine 1650. This Akt-mediated phosphorylation event enhances the ability of myosin 5a to interact with the actin cytoskeleton. Small interfering RNA-induced inhibition of myosin 5a and expression of dominant-negative myosin 5a attenuate insulin-stimulated glucose transport and GLUT4 translocation. Furthermore, knockdown of Akt2 or expression of dominant-negative Akt (DN-Akt) abolished insulin-stimulated phosphorylation of myosin 5a, inhibited myosin 5a binding to actin, and blocked insulin-stimulated glucose transport. Taken together, these data indicate that myosin 5a is a newly identified direct substrate of Akt2 and, upon insulin stimulation, phosphorylated myosin 5a facilitates anterograde movement of GLUT4 vesicles along actin to the cell surface.

Type 2 diabetes results from defective tissue sensitivity to insulin and subsequent impairment in insulin secretion. Insulin maintains glucose homeostasis largely by enhancing glucose uptake into muscle and adipose tissues, which is a process mediated by recruitment of the glucose transporter 4 (GLUT4) to the cell surface. Numerous studies have examined insulin signaling mechanisms leading to translocation of GLUT4 vesicles (G4Vs) to the plasma membrane, and this multiple-stepped process has been recently reviewed (38, 41). Insulin binding activates the tyrosine kinase activity of the insulin receptor, leading to the rapid phosphorylation of a number of substrate proteins. This triggers the activation of multiple pathways, such as the phosphatidylinositol (PI) 3-kinase-dependent signaling cascade. Downstream of PI 3-kinase, two major serine/threonine protein kinases, Akt (protein kinase B) and protein kinase Cλ (PKCλ), are activated and contribute to insulin regulation of GLUT4 translocation and glucose uptake.

Akt is an important mediator of the biological functions of insulin. Krook et al. reported that insulin-stimulated Akt phosphorylation was impaired in insulin-resistant Goto-Kakizaki rats and in muscle biopsies from type 2 diabetic patients (23). Impaired activation of Akt in response to insulin has also been described in insulin-resistant human (33) and rodent (4) adipocytes, and impaired GLUT4 translocation was associated with the defective Akt phosphorylation at insulin-resistant states (4). Furthermore, in knockout animals, targeted disruption of the Akt2 (protein kinase Bβ) gene causes insulin resistance and a type2 diabetes-like phenotype (5). Recently, several lines of evidence have demonstrated the importance of Akt for insulin-stimulated GLUT4 translocation. Thus, constitutively active membrane-targeted Akt induced GLUT4 translocation in the absence of insulin (21, 22), whereas expression of dominant-negative mutants and microinjection of blocking antibodies against Akt inhibited insulin-induced GLUT4 translocation (21, 42, 44). Using small interfering RNA (siRNA) to reduce the expression level of Akt, knockdown of Akt2 in adipocytes prevented insulin-induced GLUT4 translocation (17, 21, 42).

In an earlier study, we showed insulin stimulation can activate atypical PKCλ, which facilitates exocytosis of GLUT4 towards the plasma membrane along the microtubule system (14). We further showed that this involves Rab4 and the motor protein KIF3. However, GLUT4 proteins cannot travel along microtubules all the way to the plasma membrane. Rather, microtubule cargo interacts with the submembranous actin cytoskeletal network (45) to carry out the final stages of GLUT4 translocation. Thus, in the current study, we have focused our attention on the motor proteins which facilitate GLUT4 translocation along actin filaments (F-actin). Since insulin-induced activation of Akt is a necessary step in GLUT4 translocation, we assessed whether an actin-based motor protein might be a target of Akt. This study shows that the motor protein myosin 5a is a direct target of Akt and facilitates in the process of insulin-stimulated GLUT4 translocation along the actin network in 3T3-L1 cells.

MATERIALS AND METHODS

Materials. The HA-GLUT4-eGFP construct containing hemagglutinin (HA) in the first exofacial loop and enhanced green fluorescent protein (eGFP) at the carboxyl terminus and the human transferrin receptor construct were generous gifts from T. E. McGraw (Weill Cornell Medical College, New York, NY). Adenovirus with Akt constructs was kindly gifted by Toshiyuki Obata (Tokushima University, Tokushima, Japan). Anti-insulin-regulated aminopeptidase

* Corresponding author. Mailing address: Department of Medicine (0673), University of California, San Diego, 9500 Gilman Dr., La Jolla, CA 92093-0673. Phone: (858) 534-6651. Fax: (858) 534-6653. E-mail: jolefsky@ucsd.edu.

▽ Published ahead of print on 21 May 2007.

(IRAP) antibody was kindly provided by Steven B. Waters (Metabolex Inc., Hayward, CA). Anti-phospho-Akt substrate antibody, anti-phospho-insulin receptor (Tyr1146) antibody, anti-phospho-Akt (Ser 473) antibody, anti-phospho-ERK (Thr202/Tyr204) antibody, and anti-ERK antibody were from New England BioLabs (Beverly, MA). Anti-insulin receptor antibody, anti-Akt1/2 antibody, anti-Akt1 (protein kinase Bα) antibody, anti-myosin 5a antibody, anti-Rab4 antibody, anti-myc antibody, protein A-Sepharose, protein G-Sepharose, and horseradish peroxidase-linked anti-goat antibody were from Santa Cruz Biotechnology, Inc. (Santa Cruz, CA). Anti-Akt2 antibody and anti-IRS1 antibody were from Upstate Biotechnology, Inc. (Lake Placid, NY). Anti-α-actinin antibody was from Abcam (Cambridge, MA). Horseradish peroxidase-linked anti-rabbit and anti-mouse antibodies, sheep immunoglobulin G (IgG), rhodamine- and fluorescein isothiocyanate (FITC)-conjugated anti-rabbit antibody, and Cy3-conjugated secondary antibody were obtained from Jackson Immunoresearch Laboratories Inc. (West Grove, PA). Anti-GLUT4 antibody was from Biogenesis Inc. (Brentwood, NH). Anti-PKCλ antibody was from Transduction Laboratory (Lexington, KY). Anti-HA-11 antibody was from Covance (Princeton, NJ). Wortmannin was from Calbiochem (San Diego, CA). Dulbecco's modified Eagle medium (DMEM) and fetal calf serum were obtained from Life Technologies, Inc. (Grand Island, NY). 2-[^{3}H]Deoxyglucose and L-[^{3}H]glucose were from ICN (Costa Mesa, Calif.). All other reagents and chemicals were purchased from Sigma Chemical Co. (St. Louis, MO).

Cell treatment and transient transfection. 3T3-L1 cells were cultured and differentiated as described previously (47). For preparation of whole-cell lysates for immunoprecipitation and immunoblotting experiments, 3T3-L1 adipocytes were starved for 16 h in DMEM containing 0.1% bovine serum albumin (BSA). The cells were stimulated with or without 0.5 or 17 nM insulin at 37°C for various periods as indicated in the figures. Differentiated 3T3-L1 adipocytes were transiently transfected by electroporation, as previously described (14). For adenovirus infection, 3T3-L1 adipocytes were transduced at a multiplicity of infection of 50 PFU/cell for 16 h with the recombinant adenovirus encoding GFP or the dominant-negative form of Akt (Akt-MAA [K179M, T308A, S473A]) as described previously (21).

Generation of mutant MGT. Myc epitope-tagged COOH-terminal globular domains of myosin 5a tail (MGT) wild type and MGT-Ser1650Ala (20a) were provided by Vladimir I. Gelfand (Northwestern University, Chicago, IL). A QuikChange kit (Stratagene, La Jolla, CA) was used for site-directed mutagenesis. An oligonucleotide in which Ser 1812 of MGT was replaced with Ala was used as the primer in the in vitro mutagenesis reaction. The sequences were confirmed by direct DNA sequencing. The resulting plasmids were denoted MGT-Ser1812Ala.

RNA interference. The duplexes of each siRNA, targeting myosin 5a mRNA (target sequence, 5′-CGCUACAAGAAGCUCCAUA-3′; corresponding to the cDNA sequence from 2789 to 2807), Akt1 (18), Akt2 (target sequence, 5′-GA GAGGACCUUCCAUGUAG-3′; corresponding to the cDNA sequence from 469 to 487), PKCλ (42), and a negative control (scrambled sequence) were purchased from Dharmacon Research Inc. (Lafayette, CO). The target sequences against myosin 5a and Akt2 were chosen by a World Wide Web-based search program (www.dharmacon.com), and the absence of homology to any other gene was confirmed by a BLAST search (National Center for Biotechnology Information, National Institutes of Health). On day 8 postdifferentiation, 3T3-L1 adipocytes were electroporated with an siRNA using the Gene Pulser XCell (Bio-Rad). Electroporated cells were incubated for 48 h at 37°C prior to assays.

Immunoprecipitation and Western blotting. Coimmunoprecipitation and Western blotting experiments were performed as described previously (14). For the coimmunoprecipitation between Rab4 and myosin 5a, cells were incubated for 120 min at 4°C in phosphate-buffered saline containing 2 mM dithiobis (succinimidylpropionate) cross-linker (Pierce). Cells were lysed in a cold solubilizing buffer containing 40 mM Tris, 1 mM EGTA, 100 mM NaCl, 1 mM $MgCl_2$, 1% Nonidet P-40, 10% glycerol, 1 mM Na_3VO_4, 1 mM phenymethylsulfonyl fluoride (PMSF), and 20 mM NaF, pH 7.5. The soluble fractions were immunoprecipitated with antibodies, followed by an incubation with protein A- or protein G-conjugated beads. The immunoprecipitates were boiled with Laemmli sample buffer containing 100 mM dithiothreitol and analyzed by sodium dodecyl sulfate-polyacrylamide gel electrophoresis (SDS-PAGE) and immunoblotting.

In vitro phosphorylation of MGT. Forty-eight hours after electroporation of MGT-wild type or -Ser1650Ala into 3T3-L1 adipocytes, MGT proteins were purified using anti-c-*myc* agarose from Sigma Chemical Co. Akt2/PKBβ (delta PH, S474D) active protein and PKCλ active protein were purchased from Upstate Biotechnology, Inc., and we performed in vitro phosphorylation assays following the manufacturer's procedure. Purified MGT was incubated with 600 ng of BSA, 600 ng of recombinant Akt, or 30 ng of recombinant PKC with [γ-^{32}P]ATP (20 μCi; final ATP concentration of 100 μM per assay point). After 20 min of incubation at 30°C, the reaction was terminated by addition of Laemmli sample buffer. Samples were then analyzed by SDS-PAGE. Gels were dried, and signals were detected by using a PhosphorImager (Molecular Dynamics).

RNA isolation and RT-PCR. Forty-eight hours after electroporation of siRNA, 3T3-L1 adipocytes were scraped, and total RNA was purified with an RNeasy mini-kit from QIAGEN (Valencia, CA). The reverse transcriptional PCR (RT-PCR) was performed with a myosin 5a-specific or β-actin primer set by using a one-step RT-PCR kit from QIAGEN.

2-Deoxyglucose uptake. The procedure for evaluating glucose transport was performed as previously described (47). Glucose uptake was determined after the addition of 5 μl of substrate. 2-[^{3}H]deoxyglucose (2-DOG) or L-[^{3}H]glucose (0.1 μCi; final concentration, 0.01 mM) was added to provide a concentration at which cell membrane transport is rate limiting.

Microinjection and immunofluorescence staining. Microinjection was performed as previously described (15). Cells were incubated in complete medium for 48 h after microinjection and then serum starved for 5 h, followed by stimulation with insulin for 20 min. Immunostaining of GLUT4 was performed as described elsewhere (12). Cell surface GLUT4 staining was identified by immunofluorescence microscopy, and individual cells were scored as positive or negative for surface GLUT4. Approximately 300 cells per coverslip were counted by an observer blind to the experimental conditions. For myosin 5a immunofluorescence, we fixed and permeabilized 3T3-L1 adipocytes. The cells were then stained with polyclonal anti-myosin 5a antibody (LF-18 from Sigma Chemical Co.), followed by Cy3-conjugated anti-rabbit secondary antibody. Cy3 fluorescent emission was collected on a Nikon TE300 with a 40× 1.25-numerical-aperture oil immersion objective.

Membrane-targeting kinetics of HA-GLUT4-eGFP. Various siRNAs or MGT-wild type along with the HA-GLUT4-eGFP expression vector were electroporated together for scoring of HA-GLUT4-eGFP translocation. All images were collected on a Nikon TE300 with a 40× 1.25-numerical-aperture oil immersion objective. Simple PCI software (C-imaging Systems, Sewickley, PA) was used for image processing and quantification. In transfected cells, the intensities of the GFP and Cy3 signals were quantified, and background GFP and Cy3 fluorescence emissions were subtracted. The Cy3 fluorescence intensity for each HA-GLUT4-eGFP-expressing cell (reflecting cell surface HA-GLUT4-eGFP) was divided by the GFP fluorescence intensity (reflecting the total cellular HA-GLUT4-eGFP level) to determine the fraction of tagged GLUT4 transporter at the membrane. Translocation following insulin stimulation was expressed as a percentage of the maximum response. Fluorescence quantification was performed as previously described (30, 40).

Transferrin receptor trafficking assay. The transferrin receptor trafficking assay was a modified version of the method previously published (40). Briefly, control or myosin 5a siRNA along with the human transferrin receptor (TR) expression vector were electroporated together into 3T3-L1 adipocytes for assessment of TR translocation. The endogenous mouse TR was quenched by incubating cells for 18 h with a rat monoclonal antibody to the extracellular domain of the mouse TR but not the human TR (40). The starved cells were incubated in DMEM containing 10 μg/ml Cy3-transferrin for 2 h and stimulated with or without 170 nM insulin. The cells were fixed with 3.7% formaldehyde, and TR on the plasma membrane was stained with a monoclonal antibody directed against the extracellular domain of the human TR (Molecular Probes Inc., Eugene, OR) and detected with a FITC–anti-mouse secondary antibody. The total amount of TR expressed was determined by uptake from the medium of Cy3-labeled human transferrin (Sigma Chemical Co.; Cy3 labeling kit from Molecular Probes, Inc.). Images were taken, and total Cy3 and FITC fluorescence intensities per cell were calculated by dividing the total intensity by the area of the cell measured in pixels. To correct for background fluorescence, the same measurements were made for cells that did not express human TR. The background fluorescence intensity (for both the Cy3 and FITC fluorescence) was subtracted from the experimental data. The FITC/Cy3 ratio was calculated for each cell and averaged over 20 cells for each experiment.

Cosedimentation assay of myosin 5a-actin binding. A cosedimentation assay (29) was performed by using the nonmuscle actin binding protein Biochem kit according to the manufacturer's instructions (Cytoskeleton, Denver, CO). Briefly, starved 3T3-L1 adipocytes were stimulated with or without 17 nM insulin at 37°C for 20 min. Cells were lysed in a cold actin lysis buffer containing 20 mM Tris, 140 mM NaCl, 50 mM KCl, 2 mM $MgCl_2$, 1% Nonidet P-40, 1 mM Na_3VO_4, 1 mM PMSF, 2 mM dithiothreitol, and 50 mM NaF, pH 7.5. The soluble lysate was sedimented at 150,000 × *g* for 60 min at 20°C, and pellets were resuspended. The test protein, α-actinin, or BSA was incubated with or without

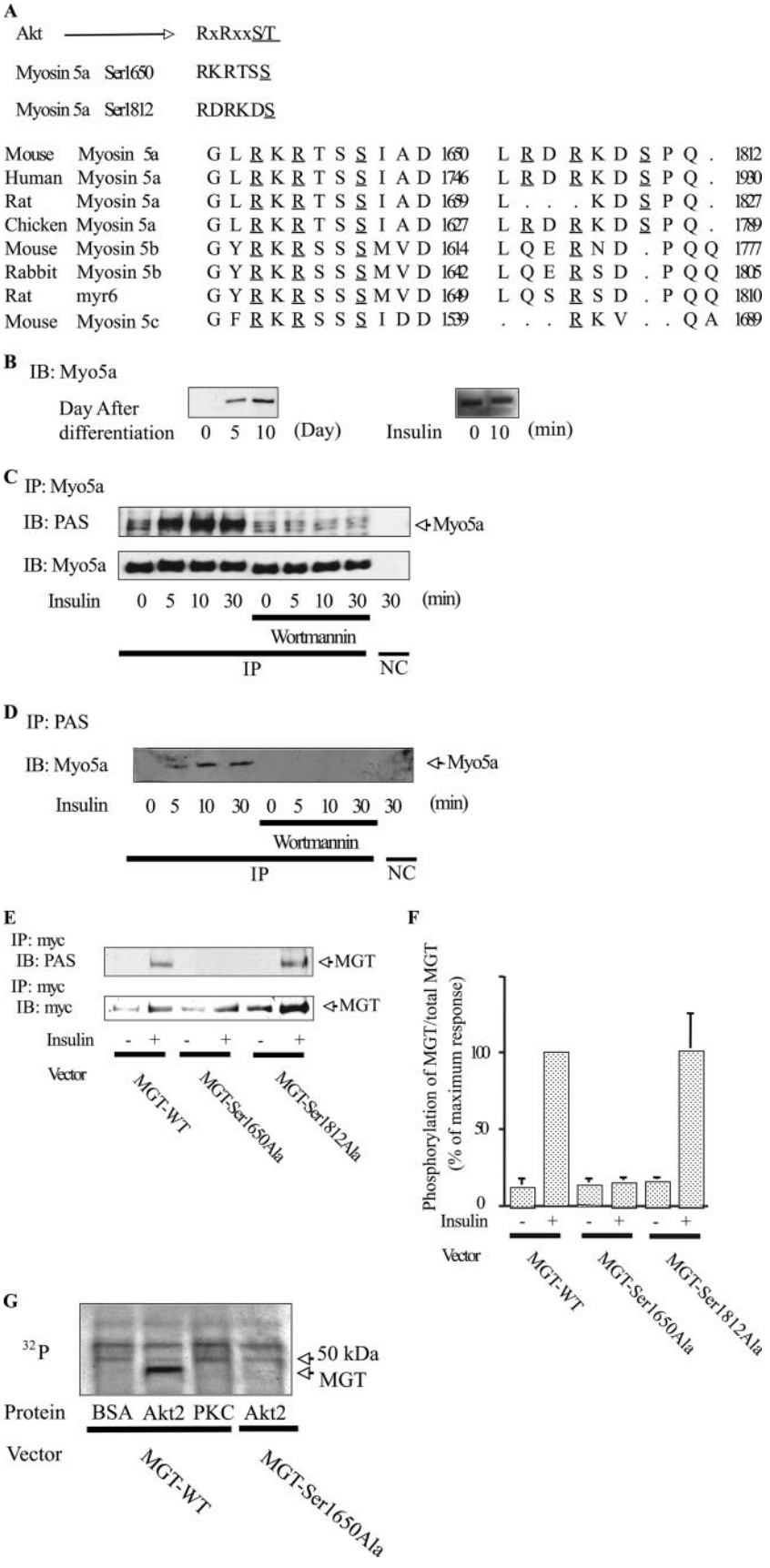
A
Akt
RxRxxS/T
Myosin 5a Ser1650
RKRTSS
Myosin 5a Ser1812
RDRKDS
Mouse Myosin 5a G L R K R T S S I A D 1680 L R D R K D S P Q . 1812
Human Myosin 5a G L R K R T S S I A D 1746 L R D R K D S P Q . 1930
Rat Myosin 5a G L R K R T S S I A D 1659 L . . . K D S P Q . 1827
Chicken Myosin 5a G L R K R T S S I A D 1627 L R D R K D S P Q . 1789
Mouse Myosin 5b G Y R K R S S S M V D 1614 L Q E R N D . P Q Q 1777
Rabbit Myosin 5b G Y R K R S S S M V D 1642 L Q E R S D . P Q Q 1805
Rat myr6 G Y R K R S S S M V D 1649 L Q S R S D . P Q Q 1810
Mouse Myosin 5c G F R K R S S S I D D 1539 . . . R K V . . Q A 1689
B
IB: Myo5a
Day After differentiation 0 5 10 (Day)
Insulin 0 10 (min)
C
IP: Myo5a
IB: PAS
Myo5a
IB: Myo5a
Insulin 0 5 10 30 0 5 10 30 30 (min)
Wortmannin
IP
NC
D
IP: PAS
IB: Myo5a
Myo5a
Insulin 0 5 10 30 0 5 10 30 30 (min)
Wortmannin
IP
NC
E
IP: myc
IB: PAS
MGT
IP: myc
IB: myc
MGT
Insulin - + - + - +
Vector
MGT-WT
MGT-Ser1650Ala
MGT-Ser1812Ala
F
Phosphorylation of MGT/total MGT (% of maximum response)
100
50
0
Insulin - + - + - +
Vector
MGT-WT
MGT-Ser1650Ala
MGT-Ser1812Ala
G
32P
50 kDa
MGT
Protein BSA Akt2 PKC Akt2
Vector
MGT-WT
MGT-Ser1650Ala

polymerized F-actin at room temperature for 30 min. The mixtures were pelleted by centrifugation at 150,000 × *g* for 1.5 h. The pellets were separated and analyzed by SDS-PAGE, and proteins were detected by immunoblotting with anti-α-actinin or anti-myosin 5a antibody or Coomassie brilliant blue (CBB) staining.

Isolation of GLUT4 vesicles. 3T3-L1 adipocytes were treated with or without 17 nM insulin for 15 min. Each cell was homogenized in buffer (25 mM HEPES, pH 7.4, 1 mM EDTA, 255 mM sucrose) supplemented with 0.1 mM Na_3VO_4, 50 mM NaF, and 1 mM PMSF, and the homogenate was centrifuged at 16,000 × *g* for 20 min. The supernatant was used for the adsorption of vesicles. Aliquots were incubated with antibody against GLUT4, followed by an incubation with protein G-conjugated beads. The immunoprecipitates were boiled with Laemmli sample buffer.

Subcellular fractionation. An abbreviated differential centrifugation procedure was used to obtain cytosol and plasma membrane fractions as previously described (6). 3T3-L1 adipocytes were homogenized in HES buffer (20 mM HEPES, pH 7.4, 1 mM EDTA, 250 mM sucrose) supplemented with 0.1 mM Na_3VO_4 and 1 mM PMSF. The homogenate was centrifuged at 19,000 × *g* for 20 min, and the resulting supernatant was centrifuged at 180,000 × *g* for 75 min at 4°C, which yielded the cytosol fraction as a supernatant. The pellet obtained on the initial spin was layered onto 1.12 M sucrose in HES buffer, followed by centrifugation at 100,000 × *g* for 60 min. This yielded a white fluffy band at the interface (plasma membrane fraction). The plasma membrane fraction was resuspended in HES and then pelleted at 40,000 × *g* for 20 min. All fractions were resuspended in HES to a final protein concentration of 1 to 2 mg/ml.

Statistics. The values are expressed as means ± standard errors. Scheffe's multiple comparison test was used to determine the significance of any differences among more than three groups. A *P* value of less than 0.05 was considered significant.

RESULTS

Insulin phosphorylates myosin 5a. Several Akt substrates have already been described, including GSK3, BAD, FOXO1, and caspase 9. Akt-induced phosphorylation of these proteins occurs in a well-defined motif, containing serine/threonine with arginine at positions −5 and −3. Therefore, we searched the myosin family sequence database (36), which revealed the presence of Akt consensus phosphorylation motifs in 10 myosin family members (Myo1b, -1c, -1f, -5a, -5b, -5c, -7a, -7b, and -15a and MYH-11). The Akt phosphorylation motif was highly consistent across all classes of myosin 5 but was not consistently represented in the other myosin classes. In particular, myosin 5a is highly expressed in mature 3T3-L1 adipocytes compared to myosin 5b and 5c (data not shown) and has two Akt consensus motifs at serines (Ser) 1650 (RKRTS*S*) and 1812 (RDRKD*S*), which were highly conserved across mammalian species (Fig. 1A), leading us to hypothesize that myosin 5a might be a direct substrate for Akt. Myosin 5a expression was strongly induced upon adipocyte differentiation (Fig.1B), consistent with this possibility. As an initial test of this idea, we conducted gel mobility shift studies on lysates derived from basal and insulin-stimulated cells. Cell lysates were analyzed by immunoblotting with an anti-myosin 5a antibody (Fig. 1B), and insulin stimulation led to an upward mobility shift of myosin 5a, consistent with increased phosphorylation of this protein. Myosin 5a tyrosine phosphorylation could not be detected with antiphosphotyrosine antibodies (data not shown), suggesting that this mobility shift was due to serine/threonine phosphorylation. To directly assess this, we utilized a phospho-Akt substrate-specific antibody to blot immunoprecipitated myosin 5a. As seen in Fig. 1C, insulin treatment led to a clear time-dependent increase in myosin 5a phosphorylation, at one or both of the Akt phosphorylation sites, and these phosphorylation events were completely blocked by treatment of the cells with the PI 3-kinase inhibitor wortmannin. When cell lysates were immunoprecipitated with the anti-phospho-Akt substrate antibody, followed by immunoblotting with myosin 5a antibody (Fig. 1D), an insulin-induced, PI 3-kinase-dependent increase in myosin 5a immunoprecipitation was detected.

To localize the site(s) of phosphorylation, we expressed myc epitope-tagged COOH-terminal globular domains of myosin 5a tail MGT (20a) in 3T3-L1 cells. The MGT constructs used were either wild type (MGT-WT) or carried serine-to-alanine mutations of either of the two possible serine phosphorylation sites at positions 1650 (MGT-Ser1650Ala) or 1812 (MGT-Ser1812Ala). We then treated the cells with insulin and compared insulin-induced phosphorylation of the wild-type and mutant MGT proteins. As seen in Fig. 1E and F, MGT-WT and MGT-Ser1812Ala were readily phosphorylated, whereas MGT-Ser1650Ala was not. To determine whether myosin 5a is a direct substrate for Akt, we purified MGT-WT and MGT-Ser1650Ala and then incubated them with purified active Akt2 or PKCλ and [γ-^{32}P]ATP. As seen in Fig. 1G, MGT-WT phosphorylation was substantially increased by active recombinant Akt2, but not by active PKCλ or control buffer. Furthermore, active Akt2 did not phosphorylate MGT-Ser1650Ala (Fig. 1G), consisted with the results in Fig. 1E and F. These results indicate that myosin 5a is a direct substrate of activated Akt and that the relevant insulin-induced phosphorylation occurs at Ser1650.

FIG. 1. Akt phosphorylates myosin 5a. (A) Akt consensus phosphorylation motif and partial amino acid sequence of mouse myosin 5a compared with human myosin 5a, rat myosin 5a, chicken myosin 5a, mouse myosin 5b, rabbit myosin 5b, rat myosin 5b (myr6), and mouse myosin 5c. Underlined regions denote amino acid sequences required for phosphorylation by Akt. (B) Myosin 5a expression is induced upon adipocyte differentiation, and insulin caused a retarded gel mobility shift of myosin 5a. On the indicated days after differentiation, 3T3-L1 cells were stimulated with or without 17 nM insulin for 10 min. The gel mobility shifts were determined by immunoblotting (IB) with anti-myosin 5a antibody. (C and D) Insulin phosphorylates myosin 5a in a wortmannin-sensitive manner. 3T3-L1 adipocytes were pretreated with or without 100 nM wortmannin and incubated with 17 nM insulin for the indicated times. (C) Myosin 5a was immunoprecipitated (IP) and phosphorylation was determined by immunoblotting with anti-phospho-specific Akt substrate (PAS) antibody. (D) PAS was immunoprecipitated, and myosin 5a was determined by immunoblotting with anti-myosin 5a. (E and F) Insulin phosphorylates myosin 5a at serine 1650. 3T3-L1 adipocytes, electroporated with MGT-WT, MGT-Ser1650Ala, or MGT-Ser1812Ala, were incubated with 17 nM insulin. MGT was immunoprecipitated, and phosphorylation was determined by immunoblotting with anti-PAS antibody. The membrane was stripped and reblotted with anti-myc antibody. (F) Data are presented as the percentages of phosphorylation/total MGT protein compared to insulin-stimulated MGT-WT electroporated cells and represent the means ± SEM from four independent experiments. (G) Akt2 directly phosphorylates MGT at serine 1650. The purified MGT-WT or -Ser1650Ala was incubated with BSA, active Akt2, or active PKC with [γ-^{32}P]ATP. Samples were then analyzed by SDS-PAGE. Gels were dried, and signals were detected by PhosphorImager. Myo5a, myosin 5a; NC, negative control (immunoprecipitated with control IgG).

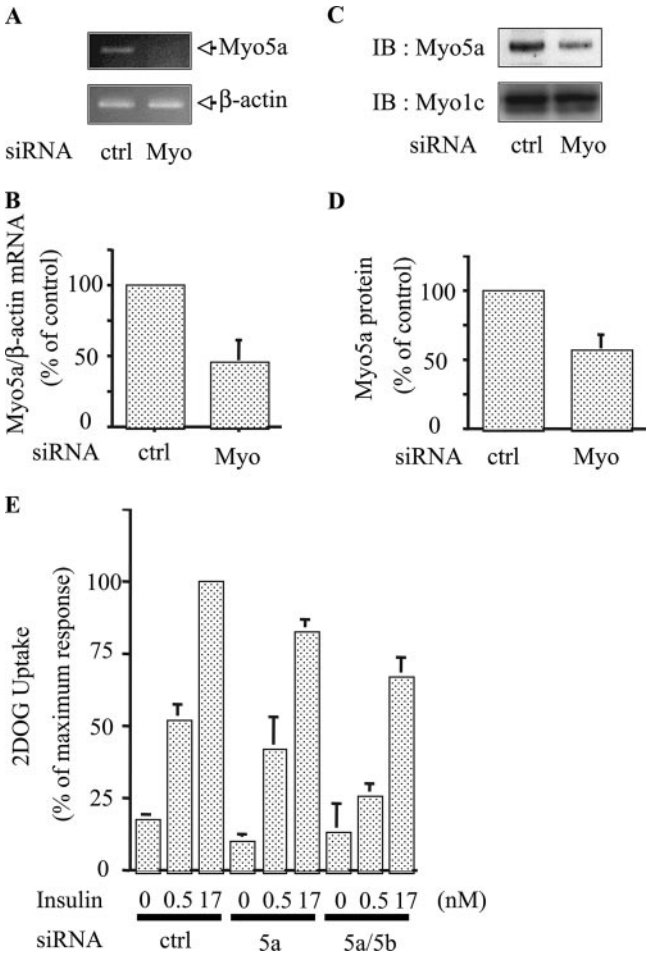

FIG. 2. Knockdown of myosin 5 reduced insulin-stimulated glucose uptake. (A and B) siRNA against myosin 5a decreased mRNA expression of myosin 5a. 3T3-L1 adipocytes were electroporated with control (ctrl) or myosin 5a (Myo) siRNA. (A) RT-PCR was performed, and the level of endogenous myosin 5a or β-actin was determined by RT-PCR with a myosin 5a-specific primer and β-actin primer. (B) Loading differences were normalized to the β-actin mRNA level, and data are presented as percentages compared to control cells. Error bars represent the means ± SEM from three independent experiments. (C and D) siRNA against myosin 5a decreased protein expression of myosin 5a. (C) At 48 hours after electroporation, cells were lysed and immunoblotting (IB) was performed with anti-myosin 5a antibody. The membrane was stripped and reblotted with anti-myosin 1c antibody. Data are presented as percentages compared to control cells and represent the mean ± SEM from three independent experiments. (E) 3T3-L1 adipocytes were electroporated with control (ctrl), myosin 5a (5a), or myosin 5a plus 5b (5a/5b) siRNA. At 48 h after electroporation, cells were stimulated with 0.5 or 17 nM insulin, and 2-DOG uptake was measured. The graph shows the mean ± SEM from five independent experiments, and the values are expressed as the percentage of maximal glucose uptake compared to that observed in insulin-stimulated control cells. Myo5a, myosin 5a; Myo1c, myosin1c.

Knockdown of myosin 5a by RNAi inhibits insulin-stimulated glucose transport. The data in Fig. 1 suggest that myosin 5a may play a role in insulin-stimulated glucose transport. To assess this, we measured 2-DOG uptake in 3T3-L1 adipocytes with and without myosin 5a depletion by RNA interference (RNAi). Several siRNAs against myosin 5a sequences were tested, and Fig. 2 shows the results for the most effective sequence obtained. At 48 h after electroporation of siMyosin 5a, we observed a 50 to 60% decrease in myosin 5a mRNA (Fig. 2A and B) and protein expression (Fig. 2C and D), compared to the levels in cells treated with scrambled siRNA. In contrast, expression levels of myosin 1c were unaffected (Fig. 2C). Myosin 5a knockdown led to a 20 to 25% decrease in insulin-stimulated glucose transport. Although this effect was modest, it should be noted that the siRNA knockdown of myosin 5a was only 50 to 60% effective. In addition, we considered the possibility that other myosin isoforms, such as myosin 5b, might compensate for the relative absence of myosin 5a (26). To assess this possibility, we used RNAi to knock down both myosin 5a and 5b, followed by measurements of 2-DOG uptake. This double knockdown led to a further decrease in insulin-stimulated 2-DOG uptake, with inhibition of glucose transport of 49 and 66% at submaximal (0.5 nM) and maximal (17 nM) insulin stimulation, respectively (Fig. 2E). We could not determine whether myosin 5b is also an Akt substrate, since antibodies which recognize this myosin isoform are not available. Furthermore, treatment of cells with siMyosin 5b or siMyosin 5c alone had no effect on glucose transport, and the combination with siMyosin 5c had no further inhibitory effect (data not shown).

Knockdown of myosin 5a or expression of dominant-negative myosin 5a inhibits insulin-stimulated GLUT4 translocation. 3T3-L1 adipocytes were microinjected with siMyosin 5a or the combination of siMyosin 5a and siMyosin 5b, followed by measurement of plasma membrane GLUT4 association by single-cell immunofluorescence with anti-GLUT4 antibody (ring assay) as previously described (12). These results showed inhibition of GLUT4 translocation by siMyosin 5a with further inhibition by the combination of siRNA treatments (Fig. 3A). We also measured GLUT4 translocation using an entirely different method (40) which relies on the transient transfection of a GLUT4 construct tagged with an HA epitope in the first extracellular loop and GFP in the intracellular C-terminal region (HA-GLUT4-eGFP). For a given cell, the magnitude of GLUT4 translocation is quantitated by normalizing the immunofluorescent labeling of the extracellular HA epitope to total cellular GFP content as previously described (30, 40). siRNA-mediated knockdown of myosin 5a inhibited insulin-stimulated redistribution of HA-GLUT4-eGFP to the cell surface (Fig. 3B), as seen by the diminished GFP ring fluorescence at the cell surface and by the decreased surface HA red fluorescence. These data are quantified in Fig. 3C, which shows that GLUT4 translocation (the surface-to-total ratio of HA-GLUT4-eGFP) in the presence of insulin was inhibited by siMyosin 5a and further inhibited by the combination of myosin 5a and 5b siRNA treatment.

To assess this concept in a different way, we expressed MGT-WT, which functions as a dominant-negative form of myosin 5 (45), along with HA-GLUT4-eGFP, and then performed single-cell GLUT4 translocation assays. Quantification of these results is shown in Fig. 3D, which clearly shows that expression of dominant-negative myosin 5a led to a 63% decrease in insulin-stimulated GLUT4 translocation. Importantly, knockdown of myosin 5a did not affect basal or insulin-stimulated surface-to-total distribution of the TR, a marker of general vesicle trafficking, showing the specificity of myosin 5a for the GLUT4 translocation system (Fig. 3E). In addition,

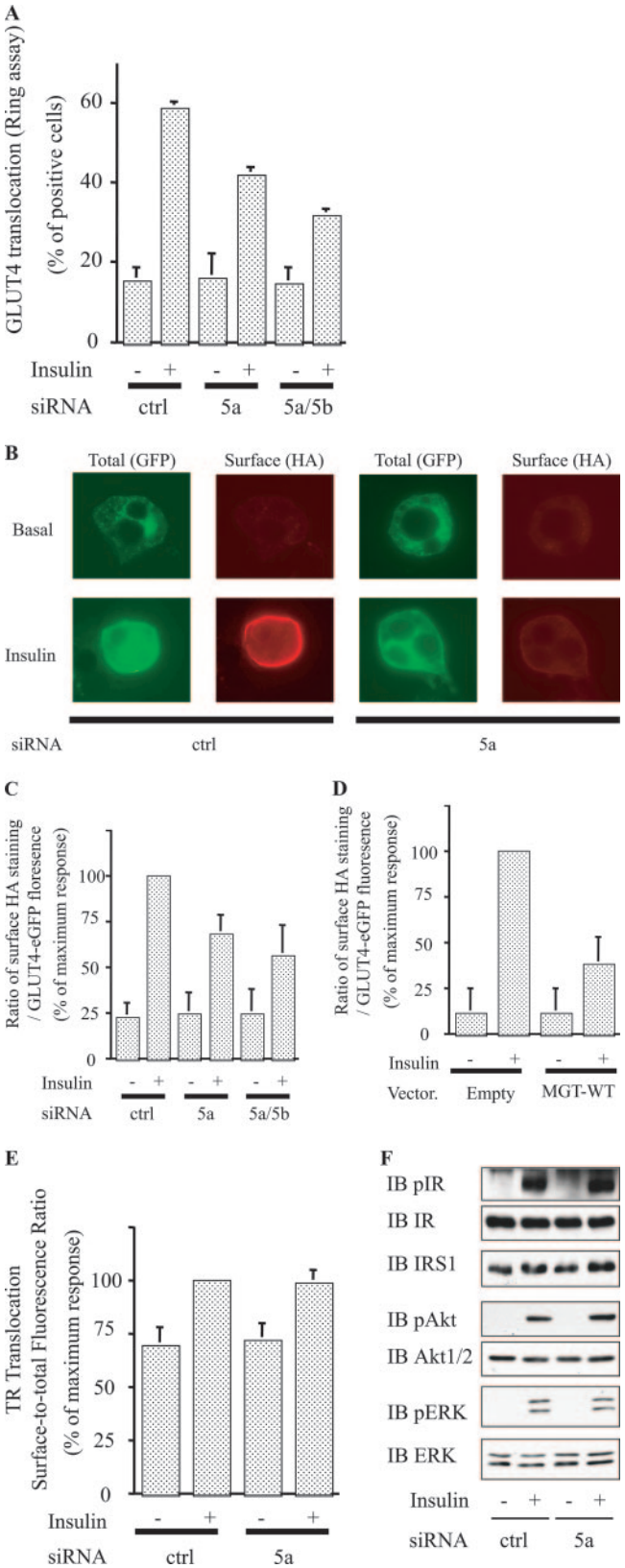

FIG. 3. Knockdown of myosin 5 or expression of MGT reduced insulin-stimulated GLUT4 translocation. (A to C) Knockdown of myosin 5 reduced insulin-stimulated GLUT4 translocation. (A) 3T3-L1 adipocytes on coverslips were microinjected with each siRNA mixture, targeting control (ctrl), myosin 5a alone (5a), or 5a and 5b combined (5a/5b). Cells were starved and stimulated with (+) or without (-) 17 nM insulin. Cell surface GLUT4 was determined by staining as described in Materials and Methods. Data shown are the mean ± SEM of results from three or four independent experiments. (B and C) 3T3-L1 adipocytes were electroporated with a dually tagged HA-GLUT4-eGFP construct with the indicated siRNA. (B) Total HA-GLUT4-eGFP expression was determined by GFP fluorescence, and HA-GLUT4-eGFP translocation to the cell surface was determined by indirect immunofluorescence of the HA in fixed cells. (C) GLUT4 translocation kinetics were assayed and analyzed as described in Materials and Methods. The data are the average ± SEM from four independent experiments (a total of 80 to 100 cells/point). (D) Expression of dominant-negative myosin 5a reduced insulin-stimulated GLUT4 translocation. MGT-wild type along with the HA-GLUT4-eGFP expression vector were electroporated together for scoring of HA-GLUT4-eGFP translocation. GLUT4 translocation kinetics were assayed and analyzed as described in Materials and Methods. The data are the average ± SEM from three independent experiments (a total of 60 to 80 cells/point). (E and F) Knockdown of myosin 5a did not affect transferrin receptor translocation or the early events in insulin signaling. Cells were electroporated with control (ctrl) or myosin 5a siRNA. At 48 h after electroporation, cells were stimulated with 170 nM insulin. (D) TR translocation was assayed and analyzed as described in Materials and Methods. The graph is the summary of data from three matched experiments in adipocytes expressing TR. The data were normalized to the surface-to-total ratio in insulin-stimulated control cells. The effects of myosin 5a knockdown on TR surface-to-total ratios were not statistically significant. (F) Western blotting was performed with the indicated antibodies. IB; immunoblot.

siMyosin5a expression had no effect on the early events of insulin signaling as demonstrated by normal levels of phosphorylation and protein expression of the insulin receptor, IRS-1, Akt, and ERK in siRNA-treated cells (Fig. 3F).

Dominant-negative Akt causes decreased phosphorylation of myosin 5a. To further explore myosin 5a phosphorylation by Akt, we examined the effect of DN-Akt (Akt-K179M/T308A/S473A). DN-Akt inhibited Akt activity in immunoprecipitations with either anti-Akt1 or -Akt2 antibody (21), indicating that DN-Akt inhibits both Akt isoforms. As shown in Fig. 4A and B, expression of DN-Akt markedly reduced insulin-stimulated myosin 5a phosphorylation, without changing myosin 5a protein levels (Fig. 4A). These data further indicate that myosin 5a is phosphorylated by Akt. Consistent with this (42), 3T3-L1 adipocytes expressing DN-Akt exhibit decreased insulin-stimulated 2-DOG uptake compared to cells transduced with control adenovirus encoding GFP (Fig. 4C).

Akt2, but not Akt1 or PKCλ, knockdown blocks insulin-induced phosphorylation of myosin 5a. To assess the specificity of Akt-mediated myosin 5a phosphorylation, we utilized siRNAs against Akt1, Akt2, and PKCλ. Thus, 3T3-L1 adipocytes were electroporated with these different siRNAs, and 48 h later insulin-stimulated myosin 5a phosphorylation was determined. Each individual siRNA led to marked depletion of the target protein (Fig. 5A and B), but as seen in Fig. 5A and C, only Akt2 knockdown inhibited insulin-induced myosin 5a phosphorylation. Taken together with the in vitro phosphorylation data in Fig. 1G, these results demonstrate the specificity of insulin-directed Akt2 activity towards myosin 5a, whereas the other PI 3-kinase-dependent insulin target proteins (Akt1 and PKCλ) did not participate in this phosphorylation event. In addition, Fig. 5D shows that knockdown of Akt2 inhibited

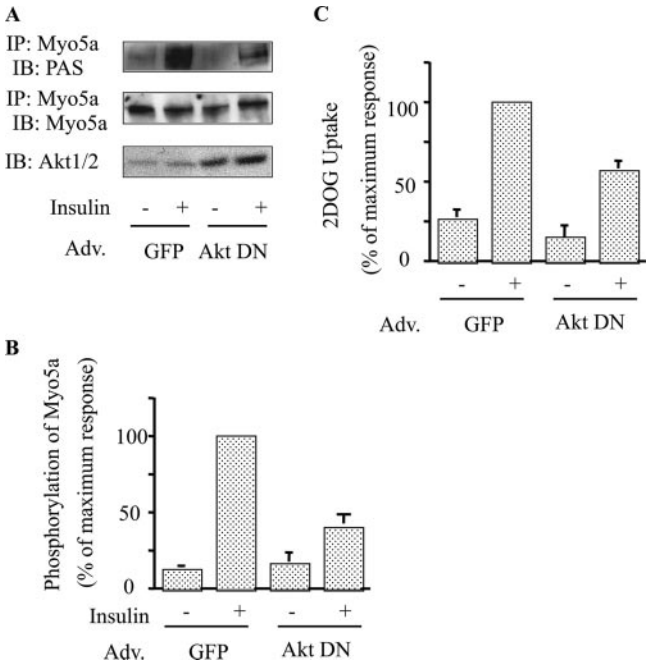

FIG. 4. Dominant-negative Akt decreased phosphorylation of myosin 5a. (A and B) Overexpression of DN-Akt decreased insulin-stimulated phosphorylation of myosin 5a. The differentiated 3T3-L1 adipocytes infected with control adenovirus (GFP) or dominant-negative Akt adenovirus (Akt DN) were stimulated with (+) or without (-) 17 nM insulin. The infected cells were lysed, and Western blotting was performed with anti-Akt1/2 antibody. The same lysates were subjected to immunoprecipitation (IP) with anti-myosin 5a antibody. Phosphorylation was detected with anti-PAS antibody (A). (B) Data are presented as percentages of phosphorylation compared to insulin-stimulated GFP-infected cells and represent the mean ± SEM from three independent experiments. (C) Overexpression of dominant-negative Akt inhibited insulin-stimulated glucose uptake. The infected cells were stimulated with (+) or without (-) 17 nM insulin. 2-Deoxyglucose uptake was measured as described in Materials and Methods. The graph shows the mean ± SEM from four independent experiments, and the values are expressed as percentages of maximal glucose uptake compared to those observed in insulin-stimulated control cells. Adv, adenovirus; IB, immunoblot.

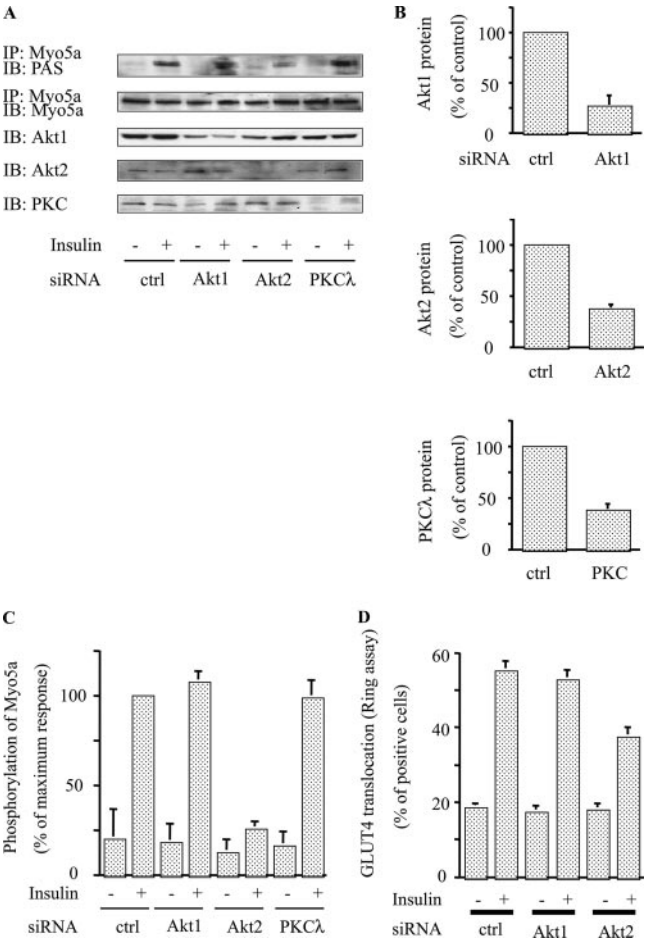

FIG. 5. Akt2, but not Akt1 or PKCλ, knockdown abolished phosphorylation of myosin 5a. (A to C) Knockdown of Akt2 decreased insulin-stimulated phosphorylation of myosin 5a. 3T3-L1 adipocytes were electroporated with the indicated siRNA, starved, and incubated in the absence (-) or presence (+) of 17 nM insulin. Then, the cells were lysed and Western blotting was performed with anti-Akt1, anti-Akt2, and anti-PKCλ antibodies. The same lysates were subjected to immunoprecipitation (IP) with anti-myosin 5a antibody. The washed immunoprecipitation products were analyzed by Western blotting with anti-PAS antibody. The membrane was stripped and reblotted with anti-myosin 5a antibody (A). (B) Data are presented as percentages of protein content compared to control siRNA-electroporated cells and represent the mean ± SEM from three independent experiments. (C) Data are presented as percentages of phosphorylation compared to insulin-stimulated control siRNA-electroporated cells and represent the mean ± SEM from three independent experiments. (D) Knockdown of Akt2 decreased insulin-stimulated GLUT4 translocation. The microinjected cells were stimulated with (+) or without (-) 17 nM insulin. Cell surface GLUT4 was determined by staining as described in Materials and Methods. Data shown are the mean ± SEM of results from three independent experiments. IB; immunoblot.

insulin-stimulated GLUT4 translocation, whereas knockdown of Akt1 had only marginal effects. As mentioned earlier, we have previously demonstrated that depletion, or inhibition, of PKCλ causes decreased insulin-stimulated GLUT4 translocation (14, 42), but this mechanism relates to proximal GLUT4 movement towards the cell surface along microtubules prior to engagement of the actin cytoskeleton (14).

Myosin 5a phosphorylation induces binding to F-actin. To assess myosin 5a function, we used a cosedimentation assay (43) to determine whether Akt-induced myosin 5a phosphorylation could facilitate binding of myosin 5a to F-actin. Since activated motor proteins can physically bind to F-actin, we incubated cell lysates from the different experimental conditions with highly purified F-actin, followed by differential sedimentation. As a positive control, the actin cosedimentation assays were also performed using α-actinin, which is known to cosediment with F-actin, and this is demonstrated in Fig. 6A. After incubation of the resuspended pellets with or without F-actin, the associated proteins were pelleted and analyzed by SDS-PAGE with either anti-myosin 5a antibody immunoblotting or CBB staining. In the absence of F-actin, myosin 5a was not detected in the pellets (Fig. 6B), whereas in the presence of F-actin, insulin stimulation led to marked cosedimentation of myosin 5a with F-actin as detected by myosin 5a immunoblotting or CBB staining. As seen in Fig. 6C and D, this ability of insulin to induce myosin 5a binding to F-actin was blocked when Akt activity was inhibited by expressing dominant-nega-

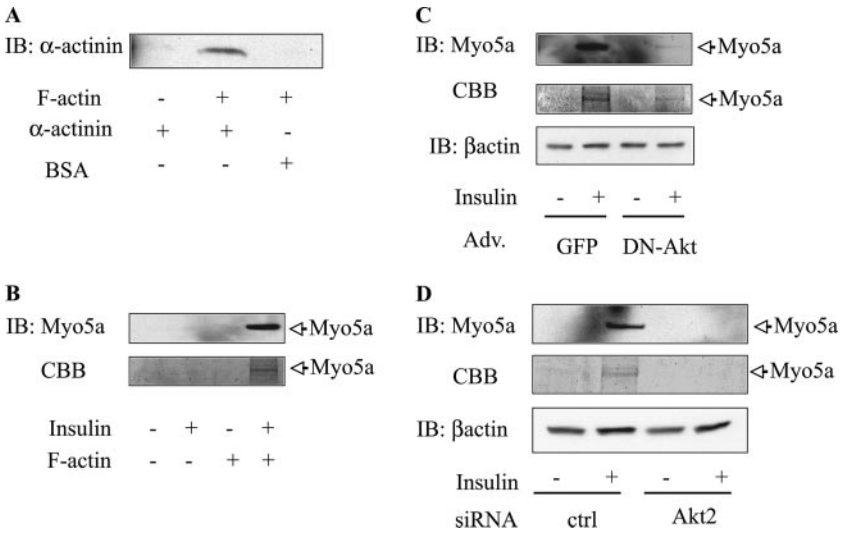

FIG. 6. Inhibition of Akt2 decrease in myosin 5a binding to actin. (A) α-Actinin bound F-actin. α-Actinin or BSA was incubated alone or with F-actin. After incubation, bundled F-actin and its associated proteins were cosedimented, and pellets were examined by SDS-PAGE and immunoblotted with antiactinin antibody. (B) Starved 3T3-L1 adipocytes were stimulated with (+) or without (-) 17 nM insulin, and sedimented lysates were incubated with or without F-actin. The mixtures were cosedimented, then pellets were examined by SDS-PAGE, and proteins were detected by immunoblotting (IB) with anti-myosin 5a antibody and CBB. (C and D) Overexpression of DN-Akt or knockdown of Akt2 abolished insulin-stimulated myosin 5a binding to F-actin. Infected (C) or electroporated (D) cells were stimulated with (+) or without (-) 17 nM insulin and then sedimented. After incubation with F-actin, cosedimented pellets were separated, analyzed by SDS-PAGE, and immunoblotted with anti-myosin 5a antibody or CBB.

tive Akt in the cells, or when Akt2 was depleted by Akt2 siRNA.

Insulin leads to myosin 5a binding to GLUT4-containing vesicles and translocation to the plasma membrane. Our data indicate that the Akt-mediated phosphorylation of myosin 5a is directly involved in the movement of G4Vs to the cell surface along F-actin. From this, we predicted that myosin 5a would be associated with G4Vs. To test this idea, we purified G4Vs and examined their association with myosin 5a. As previously reported, these vesicles contain IRAP, which colocalized with GLUT4 (Fig. 7A), and translocated to the plasma membrane in response to insulin (35). As seen in Fig. 7A, insulin treat-

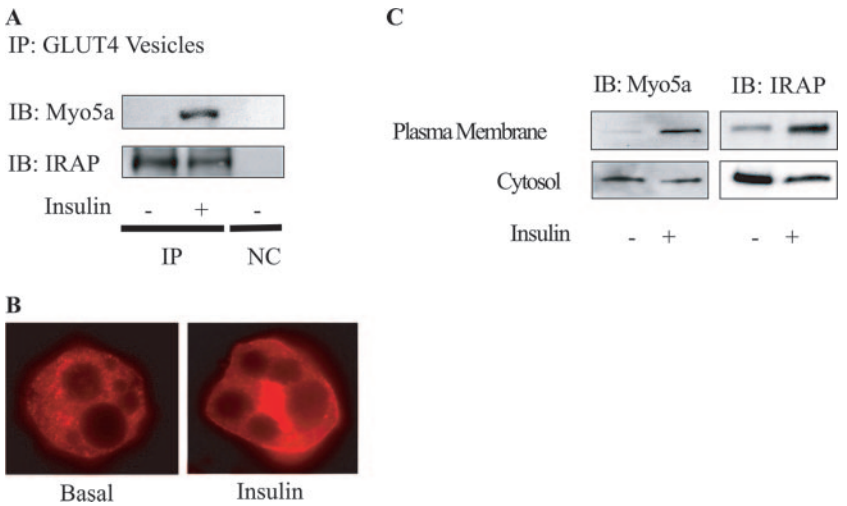

FIG. 7. Insulin leads to myosin 5a binding to GLUT4-containing vesicles and translocation to the plasma membrane. (A) Insulin-stimulated myosin 5a associated with GLUT4-containing vesicles. Starved 3T3-L1 adipocytes were stimulated with (+) or without (-) 17 nM insulin, and then GLUT4-containing vesicles were collected as described in Materials and Methods. The immunoprecipitates were analyzed by SDS-PAGE and immunoblotted (IB) with indicated antibodies. (B and C) Myosin 5a and IRAP translocated to the plasma membrane upon insulin stimulation. (B) Starved 3T3-L1 adipocytes were stimulated with (insulin) or without (basal) 17 nM insulin and then fixed and immunostained with anti-myosin 5a antibody, followed by incubation with rhodamine-conjugated secondary antibody. Localization of myosin 5a was examined using confocal microscopy. (C) Starved 3T3-L1 adipocytes were stimulated with (+) or without (-) 17 nM insulin, each fraction was separated by ultracentrifugation as described in Materials and Methods, and Western blotting was performed with anti-myosin 5a or anti-IRAP antibody. IP, immunoprecipitated; Myo5a, myosin 5a; NC, negative control (immunoprecipitated with control IgG).

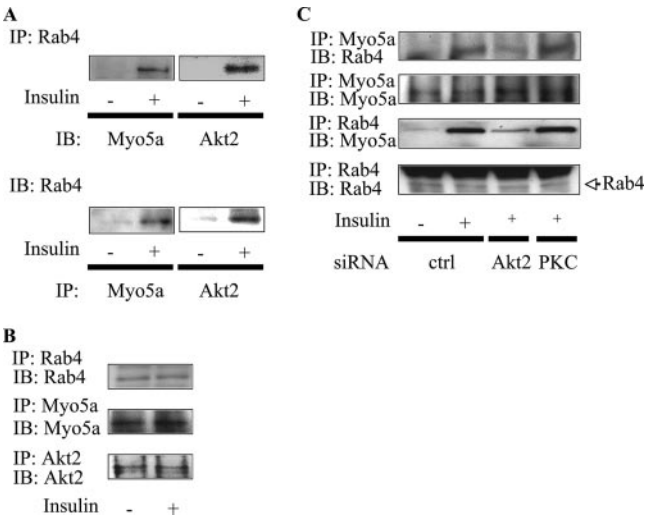

FIG. 8. Association between myosin 5a, Akt2, and Rab4. (A and B) Rab4 associated with myosin 5a and Akt2. 3T3-L1 adipocytes were serum starved and incubated with 17 nM insulin. The cells were lysed and immunoprecipitated (IP) with the anti-Rab4, anti-myosin 5a, or anti-Akt2 antibodies. The washed immunoprecipitation products were analyzed by immunoblotting (IB) with the indicated antibodies. (B) The membrane was stripped and reblotted with anti-myosin 5a, anti-Akt2, or anti-Rab4 antibodies. These experiments were repeated three or four times. (C) Insulin-stimulated interaction of myosin 5a and Rab4 is downstream of the Akt2 pathway. 3T3-L1 adipocytes were electroporated with the indicated siRNA, starved, and incubated in the absence (-) or presence (+) of 17 nM insulin. Then, the cells were lysed and immunoprecipitated with anti-Rab4 or anti-myosin 5a antibodies. The washed immunoprecipitation products were analyzed by immunoblotting with the indicated antibodies. The membrane was stripped and reblotted with anti-myosin 5a or anti-Rab4 antibodies. Myo5a, myosin 5a.

ment led to the association of myosin 5a with G4Vs. Furthermore, upon insulin stimulation, myosin 5a shifted from the cytosol to the plasma membrane, as shown by examining myosin 5a immunofluorescence (Fig. 7B). This was confirmed by subcellular fractionation studies (Fig. 7C), which showed that insulin stimulation led to a measurable decrease in cytosolic myosin 5a and a large increase in plasma membrane myosin 5a, comparable to the results for IRAP translocation (Fig. 7C). These data further support the concept that myosin 5a plays a role in insulin-stimulated GLUT4 translocation to the plasma membrane.

Association between myosin 5a, Akt, and Rab4. Since Akt can phosphorylate myosin 5a, we investigated whether Akt2 can be detected in myosin 5a coimmunoprecipitation experiments but found no evidence for Akt1 or Akt2 association with myosin 5a (data not shown). Since we have previously shown that another motor protein, KIF3, can interact with the small GTP binding protein Rab4 following insulin stimulation (14), we assessed whether myosin 5a could also interact with Rab4. In response to insulin stimulation, myosin 5a coprecipitated with Rab4 (Fig. 8A). This was observed when Rab4 immunoprecipitates were immunoblotted with myosin 5a antibody or when myosin 5a immunoprecipitates were immunoblotted with Rab4 antibody (Fig. 8A). Interestingly, insulin also increased coimmunoprecipitation of Rab4 with Akt2 (Fig. 8A), whereas no Rab4 could be detected in Akt1 immunoprecipitates (data not shown). The same amounts of myosin 5a, Akt2, and Rab4 were detected in each immunoprecipitate (Fig. 8B). Binding of Rab4 to myosin 5a was decreased in Akt2 knockdown cells but not in PKCλ knockdown cells (Fig. 8C), while neither Akt2 nor PKCλ knockdown affected the amount of myosin 5a and Rab4. These data indicate that the insulin-stimulated interaction of myosin 5a and Rab4 is downstream of Akt2.

DISCUSSION

Myosin 5 is a ubiquitously expressed non-muscle-type F-actin-interacting motor protein. There are three distinct subclasses (myosin 5a, -b, and -c) in vertebrates, which are differentially expressed with overlapping functions (1, 46). These isoforms are dimeric molecules, containing two conserved motor domains followed by six repeats of an IQ motif and two tail domains which participate in cargo binding. Myosin 5a plays an important role in anterograde membrane trafficking in specific transport pathways, such as melanosomes (9), neurotransmitter vesicles (34), and insulin-containing vesicles (43). In the current study, we report that myosin 5a/5b play a role in anterograde GLUT4 vesicle trafficking in 3T3-L1 adipocytes. Our data further show that myosin 5a is a direct target for insulin-directed Akt2 activity and that insulin-induced myosin 5a phosphorylation stimulates its ability to interact with F-actin, consistent with its role as an actin cytoskeletal-based motor protein facilitating GLUT4 exocytosis.

Although the functional regulation of myosin 5 is incompletely understood, two major domains are known to participate in the motor activity of myosin 5a. A series of repeat IQ motifs are located near the motor protein head domain, and these motifs bind to calmodulins and specific myosin light chains (36). The myosin 5a tail domain is important for cargo binding and cellular localization, and overexpression of this tail domain can inhibit myosin 5a activity (45). Interestingly, by searching the myosin sequence databases, we observed that the myosin 5a tail domain contains two Akt substrate sequence repeats (RXRXXpS/T) at Ser 1650 and Ser 1812. Here we used three distinct approaches to test whether myosin 5a is a direct substrate of Akt. First, we showed a modest insulin-stimulated gel mobility shift of myosin 5a (Fig. 1B). Second, we utilized a phospho-Akt substrate-specific antibody and clearly demonstrated insulin-stimulated phosphorylation of Ser 1650 in a PI 3-kinase- and Akt2-dependent manner. Third, we purified the myosin 5a C-terminal domain (MGT) and used a direct in vitro phosphorylation assay to demonstrate that Akt2 phosphorylates myosin 5a at Ser 1650. Further, insulin-induced phosphorylation of myosin 5a stimulated the actin binding activity of this protein, and this insulin effect was inhibited by expression of dominant-negative Akt, or siRNA-mediated Akt2 knockdown, as well as expression of dominant-negative mutant myosin 5a. Insulin stimulation also caused association of myosin 5a with GLUT4 vesicles and translocation of myosin 5a to the plasma membrane along with GLUT4 and IRAP. Consistent with the motor function of myosin 5a, we found that siRNA-induced depletion of myosin 5a, or expression of dominant-negative myosin 5a, inhibited insulin-stimulated glucose transport and GLUT4 translocation without affecting the early steps of insulin signaling. From these results, we conclude that insulin induces myosin 5a activation via Akt2-mediated phos-

phorylation of Ser 1650 in the tail domain. In turn, activated myosin 5a then functions as a motor protein facilitating anterograde translocation of GLUT4 through the actin cytoskeleton network.

Activation of insulin receptor is rapidly followed by docking of insulin receptor substrates and stimulation of PI 3-kinase. Akt and PKCλ are serine/threonine kinases activated downstream of PI 3-kinase, and both are mediators of major metabolic actions of insulin, such as glucose transport and GLUT4 translocation (38). However, the signaling events downstream of these two kinases remain to be fully elucidated. Recently, a new Akt substrate, Akt substrate of 160 kDa (AS160), has been identified (19). Upon insulin stimulation, phosphorylation of AS160 through Akt leads to inactivation of AS160 GAP activity, which releases retention of GLUT4, promoting translocation (7, 28). Evidence shows that Rab8A and Rab14 are targets of AS160 and may be involved in GLUT4 translocation in the perinuclear region (16). That report suggested that AS160 serves as a modulator of basal GLUT4 trafficking. More recently, Gonzalez et al. reported that inhibition of Akt impaired GLUT4 exocytosis in AS160 knockdown adipocytes, suggesting that additional Akt substrates, other than AS160, are involved in insulin regulation of GLUT4 exocytosis (8). They also showed that Akt activity was specifically required for GLUT4 exocytosis within the region 250 nm from the plasma membrane, where F-actin is located in juxtaposition to the plasma membrane. These data are fully consistent with our results showing that myosin 5a is a new Akt2 substrate involved in GLUT4 translocation along F-actin.

It has been well demonstrated in several systems that vesicular trafficking is observed along microtubule and actin cytoskeletal structures (10, 27). Indeed, in adipocytes, disruption of microtubules (11, 24, 31) or F-actin (20) resulted in marked inhibition of insulin-stimulated GLUT4 translocation and glucose uptake. Since the plus ends of microtubules do not connect directly to the plasma membrane, vesicle cargo has to be transferred from microtubules to F-actin structures in order to reach the cell surface. Although the understanding of vesicle transfer mechanisms between these two systems is limited, it has been reported that melanosomes can be transported to melanocyte dendrites by the microtubule-based motor protein KIF3 and that the subsequent movement of these vesicles, and their tethering at the cell membrane, is dependent on myosin 5 and F-actin (46). Further support for this microtubule/actin cytoskeletal "handoff" model has been provided by colocalization and binding studies that showed the direct interaction between the myosin 5a and KIF3 tail domains (13). Close cooperation between the kinesin/microtubule and myosin 5/F-actin systems has also been observed in melanophore transport (32). In our previous study, we found that GLUT4 vesicles are localized to the perinuclear Golgi region in nonstimulated cells and, after insulin stimulation, are transported in an anterograde fashion along microtubules, and this is dependent on the microtubule-based kinesin motor protein KIF3 (14). In the overall process of GLUT4 exocytosis, this would account for GLUT4 movement along microtubules towards the cell periphery after insulin stimulation. The potential transfer mechanism of GLUT4 vesicles from microtubules to the F-actin system has not been addressed, and based on the current results, we suggest that PI 3-kinase-dependent KIF3/microtubule and myosin 5a/F-actin cooperation could be a model to translocate GLUT4 vesicles from their intracellular perinuclear loci to the plasma membrane via microtubular and then F-actin structures, under the influence of insulin.

Previous reports have shown that another microtubule motor protein, KIF5B, and the actin-based motor protein, myosin 1c, are involved in insulin-induced GLUT4 translocation (2, 37). In this regard, KIF5B was wortmannin insensitive, suggesting that a PI 3-kinase-independent pathway(s) mediates insulin's effect on this protein. Additionally, myosin 1c is now thought to facilitate the fusion of exocytic GLUT4-containing vesicles with the adipocyte plasma membrane (3). Time-lapse total internal reflection microscopy studies (25) in rat primary adipocytes demonstrated that GLUT4 vesicles rapidly move along microtubules, periodically tethering to the plasma membrane in the basal state, and that insulin halted this traffic by enhancing the tethering step. It is possible that myosin 5a participates in this tethering step.

Akt and PKCλ are both PI 3-kinase-dependent serine/threonine kinases, and numerous studies have demonstrated that both PKCλ and Akt are necessary for insulin-induced glucose transport (14, 17, 21, 22, 42, 44). These findings raise the question as to how these two similar serine/threonine kinases both play important roles in the process of insulin signaling to glucose transport. The current study, coupled with our previous reports of PKCλ signaling (14), provide a working model to help understand these phenomena. In a previous study, we reported that insulin stimulation of PKCλ mediates the activation of a kinesin family motor protein, KIF3, to facilitate anterograde movement of GLUT4 along microtubule structures. In the current study, we find that insulin-induced Akt2 activation stimulates the ability of another motor protein, myosin 5a, to mediate anterograde movement of GLUT4 by the actin cytoskeleton. This suggests that sequential cooperation of PKCλ/KIF3 and Akt2/myosin 5a could participate in the movement of GLUT4 cargo through the microtubule system and then on through the actin cytoskeleton, thus providing an explanation for the role of both of these serine/threonine kinases in the overall process of GLUT4 translocation. Additional supporting evidence for this idea is the subcellular localization of these two kinases. Thus, PKCλ has been colocalized with microtubules (32), whereas Akt is colocalized with F-actin (39). Taken together, these differences in subcellular localizations of Akt and PKCλ, combined with the biochemical and biological data in the current and previous studies, are consistent with the working model proposed above.

The PKCλ/KIF3/microtubule and Akt2/myosin 5a/actin systems are biochemically and structurally distinct. Nevertheless, GLUT4 vesicles must be recognized by both systems under the influence of insulin to complete the full process of GLUT4 translocation from its initial perinuclear localization to the cell surface. Although the mechanisms for this remain incompletely understood, we have provided some evidence for a possible linker protein between GLUT4 vesicles and both KIF3 and myosin 5a motor proteins. Thus, we have previously shown that insulin stimulates Rab4 activation in 3T3-L1 adipocytes and that Rab4 may serve as an adaptor, between KIF3 and GLUT4 vesicles, in relationship to microtubule-based movement (14). In the current study, we show that, under the influence of insulin, myosin 5a binds to GLUT4-containing

vesicles and translocates to the plasma membrane. In the insulin-stimulated state, Rab4 can also coassociate with myosin 5a. This Rab4 association with myosin 5a was decreased in Akt2 knockdown but not in PKCλ knockdown cells, suggesting that the insulin-stimulated interaction of myosin 5a and Rab4 is downstream of Akt2. Thus, Rab4 may provide a common link between GLUT4 vesicles and the microtubular and actin-based motor proteins facilitating the transfer of GLUT4 vesicles from microtubules to the F-actin system in the process of GLUT4 translocation.

In summary, these results provide evidence that the actin-based motor protein myosin 5a is a direct substrate for insulin-stimulated Akt2. In turn, Akt2-dependent phosphorylation of myosin 5a enhances its ability to interact with the actin cytoskeleton and GLUT4 vesicles, and depletion of myosin 5a inhibits glucose transport stimulation. As such, these novel results are consistent with the view that myosin 5a is a new regulator of GLUT4 translocation, providing an important and direct functional link between the insulin-directed PI 3-kinase–Akt2 signaling pathway and GLUT4 translocation. In addition, taken together with our previous findings on the connection between activation of PKCλ and the microtubule-based motor protein KIF3, it is suggested that PKCλ and Akt2 sequentially cooperate to translocate GLUT4 vesicles from the perinuclear pool to the cell surface through a sequential KIF3/microtubule and myosin 5a/F-actin mechanism.

ACKNOWLEDGMENTS

We are grateful to Vladimir I. Gelfand for MGT wild-type and Ser1650Ala mutant constructs, T. E. McGraw for HA-GLUT4-eGFP and human transferrin receptor constructs, Steven B. Waters for anti-IRAP antibody, John A. Mercer for constructs, Mitsunori Fukuda for constructs, and Toshiyuki Obata for adenovirus with Akt constructs. DNA sequencing was performed by the DNA Shared Resource, UCSD Cancer Center, which is funded in part by NCI Cancer Center support grant 2 P30 CA23100-18. We thank Elizabeth J. Hansen for editorial assistance.

This study was funded in part by National Institutes of Health grant DK 33651 (J.M.O.) and the University of California Discovery Program Project bio03-10383 (BioStar) with matching funds from Pfizer Incorporated.

REFERENCES

1. **Bement, W. M., T. Hasson, J. A. Wirth, R. E. Cheney, and M. S. Mooseker.** 1994. Identification and overlapping expression of multiple unconventional myosin genes in vertebrate cell types. Proc. Natl. Acad. Sci. USA **91:**11767.
2. **Bose, A., A. Guilherme, S. I. Robida, S. M. Nicoloro, Q. L. Zhou, Z. Y. Jiang, D. P. Pomerleau, and M. P. Czech.** 2002. Glucose transporter recycling in response to insulin is facilitated by myosin Myo1c. Nature **420:**821–824.
3. **Bose, A., S. Robida, P. S. Furcinitti, A. Chawla, K. Fogarty, S. Corvera, and M. P. Czech.** 2004. Unconventional myosin Myo1c promotes membrane fusion in a regulated exocytic pathway. Mol. Cell. Biol. **24:**5447–5458.
4. **Carvalho, E., C. Rondinone, and U. Smith.** 2000. Insulin resistance in fat cells from obese Zucker rats—evidence for an impaired activation and translocation of protein kinase B and glucose transporter 4. Mol. Cell. Biochem. **206:**7–16.
5. **Cho, H., J. L. Thorvaldsen, Q. Chu, F. Feng, and M. J. Birnbaum.** 2001. Akt1/PKBα is required for normal growth but dispensable for maintenance of glucose homeostasis in mice. J. Biol. Chem. **276:**38349–38352.
6. **Egawa, K., H. Maegawa, K. Shi, T. Nakamura, T. Obata, T. Yoshizaki, K. Morino, S. Shimizu, Y. Nishio, E. Suzuki, and A. Kashiwagi.** 2002. Membrane localization of 3-phosphoinositide-dependent protein kinase-1 stimulates activities of Akt and atypical protein kinase C but does not stimulate glucose transport and glycogen synthesis in 3T3-L1 adipocytes. J. Biol. Chem. **277:**38863–38869.
7. **Eguez, L., A. Lee, J. A. Chavez, C. P. Miinea, S. Kane, G. E. Lienhard, and T. E. McGraw.** 2005. Full intracellular retention of GLUT4 requires AS160 Rab GTPase activating protein. Cell Metab. **2:**263–272.
8. **Gonzalez, E., and T. E. McGraw.** 2006. Insulin signaling diverges into Akt-dependent and -independent signals to regulate the recruitment/docking and the fusion of GLUT4 vesicles to the plasma membrane. Mol. Biol. Cell **17:**4484–4493.
9. **Gross, S. P., M. A. Welte, S. M. Block, and E. F. Wieschaus.** 2002. Coordination of opposite-polarity microtubule motors. J. Cell Biol. **156:**715–724.
10. **Hirokawa, N., Y. Noda, and Y. Okada.** 1998. Kinesin and dynein superfamily proteins in organelle transport and cell division. Curr. Opin. Cell Biol. **10:**60–73.
11. **Huang, J., T. Imamura, J. L. Babendure, J. C. Lu, and J. M. Olefsky.** 2005. Disruption of microtubules ablates the specificity of insulin signaling to GLUT4 translocation in 3T3-L1 adipocytes. J. Biol. Chem. **280:**42300–42306.
12. **Huang, J., T. Imamura, and J. M. Olefsky.** 2001. Insulin can regulate GLUT4 internalization by signaling to Rab5 and the motor protein dynein. Proc. Natl. Acad. Sci. USA **98:**13084–13089.
13. **Huang, J. D., S. T. Brady, B. W. Richards, D. Stenolen, J. H. Resau, N. G. Copeland, and N. A. Jenkins.** 1999. Direct interaction of microtubule- and actin-based transport motors. Nature **397:**267–270.
14. **Imamura, T., J. Huang, I. Usui, H. Satoh, J. Bever, and J. M. Olefsky.** 2003. Insulin-induced GLUT4 translocation involves protein kinase C-lambda-mediated functional coupling between Rab4 and the motor protein kinesin. Mol. Cell. Biol. **23:**4892–4900.
15. **Imamura, T., P. Vollenweider, K. Egawa, M. Clodi, K. Ishibashi, N. Nakashima, S. Ugi, J. W. Adams, J. H. Brown, and J. M. Olefsky.** 1999. G alpha-q/11 protein plays a key role in insulin-induced glucose transport in 3T3-L1 adipocytes. Mol. Cell. Biol. **19:**6765–6774.
16. **Ishikura, S., P. J. Bilan, and A. Klip.** 2007. Rabs 8A and 14 are targets of the insulin-regulated Rab-GAP AS160 regulating GLUT4 traffic in muscle cells. Biochem. Biophys. Res. Commun. **353:**1074–1079.
17. **Jiang, Z. Y., Q. L. Zhou, K. A. Coleman, M. Chouinard, Q. Boese, and M. P. Czech.** 2003. Insulin signaling through Akt/protein kinase B analyzed by small interfering RNA-mediated gene silencing. Proc. Natl. Acad. Sci. USA **100:**7569–7574.
18. **Jiang, Z. Y., Q. L. Zhou, J. Holik, S. Patel, J. Leszyk, K. Coleman, M. Chouinard, and M. P. Czech.** 2005. Identification of WNK1 as a substrate of Akt/protein kinase B and a negative regulator of insulin-stimulated mitogenesis in 3T3-L1 cells. J. Biol. Chem. **280:**21622–21628.
19. **Kane, S., H. Sano, S. C. Liu, J. M. Asara, W. S. Lane, C. C. Garner, and G. E. Lienhard.** 2002. A method to identify serine kinase substrates. Akt phosphorylates a novel adipocyte protein with a Rab GTPase-activating protein (GAP) domain. J. Biol. Chem. **277:**22115–22118.
20. **Kanzaki, M., and J. E. Pessin.** 2001. Insulin-stimulated GLUT4 translocation in adipocytes is dependent upon cortical actin remodeling. J. Biol. Chem. **276:**42436–42444.

20a. **Karcher, R. L., J. T. Roland, F. Zappacosta, M. J. Huddleston, R. S. Aman, S. A. Carr, and V. I. Gelfand.** 2001. Cell cycle regulation of myosin-V by calcium/calmodulin-dependent kinase II. Science **293:**1317–1320.

21. **Katome, T., T. Obata, R. Matsushima, N. Masuyama, L. C. Cantley, Y. Gotoh, K. Kishi, H. Shiota, and Y. Ebina.** 2003. Use of RNA interference-mediated gene silencing and adenoviral overexpression to elucidate the roles of AKT/protein kinase B isoforms in insulin actions. J. Biol. Chem. **278:**28312–28323.
22. **Kohn, A. D., S. A. Summers, M. J. Birnbaum, and R. A. Roth.** 1996. Expression of a constitutively active Akt Ser/Thr kinase in 3T3-L1 adipocytes stimulates glucose uptake and glucose transporter 4 translocation. J. Biol. Chem. **271:**31372–37378.
23. **Krook, A., Y. Kawano, X. M. Song, S. Efendic, R. A. Roth, H. Wallberg-Henriksson, and J. R. Zierath.** 1997. Improved glucose tolerance restores insulin-stimulated Akt kinase activity and glucose transport in skeletal muscle from diabetic Goto-Kakizaki rats. Diabetes **46:**2110–2114.
24. **Liu, L. B., W. Omata, I. Kojima, and H. Shibata.** 2003. Insulin recruits GLUT4 from distinct compartments via distinct traffic pathways with differential microtubule dependence in rat adipocytes. J. Biol. Chem. **278:**30157–30169.
25. **Lizunov, V. A., H. Matsumoto, J. Zimmerberg, S. W. Cushman, and V. A. Frolov.** 2005. Insulin stimulates the halting, tethering, and fusion of mobile GLUT4 vesicles in rat adipose cells. J. Cell Biol. **169:**481–489.
26. **Mercer, J. A., P. K. Seperack, M. C. Strobel, N. G. Copeland, and N. A. Jenkins.** 1991. Novel myosin heavy chain encoded by murine dilute coat colour locus. Nature **349:**709–713.
27. **Mermall, V., P. L. Post, and M. S. Mooseker.** 1998. Unconventional myosins in cell movement, membrane traffic, and signal transduction. Science **279:**527–533.
28. **Miinea, C. P., H. Sano, S. Kane, E. Sano, M. Fukuda, J. Peranen, W. S. Lane, and G. E. Lienhard.** 2005. AS160, the Akt substrate regulating GLUT4 translocation, has a functional Rab GTPase-activating protein domain. Biochem. J. **391:**87–93.
29. **Nascimento, A. A., R. E. Cheney, S. B. Tauhata, R. E. Larson, and M. S. Mooseker.** 1996. Enzymatic characterization and functional domain mapping of brain myosin-V. J. Biol. Chem. **271:**17561–17569.
30. **Nguyen, M. T., H. Satoh, S. Favelyukis, J. L. Babendure, T. Imamura, J. I. Sbodio, J. Zalevsky, B. I. Dahiyat, N. W. Chi, and J. M. Olefsky.** 2005. JNK

and tumor necrosis factor-alpha mediate free fatty acid-induced insulin resistance in 3T3-L1 adipocytes. J. Biol. Chem. **280:**35361–35371.

31. **Olson, A. L., A. R. Trumbly, and G. V. Gibson.** 2001. Insulin-mediated GLUT4 translocation is dependent on the microtubule network. J. Biol. Chem. **276:**10706–10714.
32. **Rodionov, V. I., A. J. Hope, T. M. Svitkina, and G. G. Borisy.** 1998. Functional coordination of microtubule-based and actin-based motility in melanophores. Curr. Biol. **8:**165–168.
33. **Rondinone, C. M., E. Carvalho, C. Wesslau, and U. P. Smith.** 1999. Impaired glucose transport and protein kinase B activation by insulin, but not okadaic acid, in adipocytes from subjects with type II diabetes mellitus. Diabetologia **42:**819–825.
34. **Rose, S. D., T. Lejen, L. Casaletti, R. E. Larson, T. D. Pene, and J. M. Trifaro.** 2003. Myosins II and V in chromaffin cells: myosin V is a chromaffin vesicle molecular motor involved in secretion. J. Neurochem. **85:**287–298.
35. **Ross, S. A., H. M. Scott, N. J. Morris, W. Y. Leung, F. Mao, G. E. Lienhard, and S. R. Keller.** 1996. Characterization of the insulin-regulated membrane aminopeptidase in 3T3-L1 adipocytes. J. Biol. Chem. **271:**3328–3332.
36. **Sellers, J. R.** 2000. Myosins: a diverse superfamily. Biochim. Biophys. Acta **1496:**3–22.
37. **Semiz, S., J. G. Park, S. M. Nicoloro, P. Furcinitti, C. Zhang, A. Chawla, J. Leszyk, and M. P. Czech.** 2003. Conventional kinesin KIF5B mediates insulin-stimulated GLUT4 movements on microtubules. EMBO J. **22:**2387–2399.
38. **Shepherd, P. R., and B. B. Kahn.** 1999. Glucose transporters and insulin action—implications for insulin resistance and diabetes mellitus. N. Engl. J. Med. **341:**248–257.
39. **Standaert, M. L., G. Bandyopadhyay, L. Perez, D. Price, L. Galloway, A. Poklepovic, M. P. Sajan, V. Cenni, A. Sirri, J. Moscat, A. Toker, and R. V. Farese.** 1999. Insulin activates protein kinases C-zeta and C-lambda by an autophosphorylation-dependent mechanism and stimulates their translocation to GLUT4 vesicles and other membrane fractions in rat adipocytes. J. Biol. Chem. **274:**25308–25316.
40. **Subtil, A., M. Lampson, S. Keller, and T. McGraw.** 2000. Characterization of the insulin-regulated endocytic recycling mechanism in 3T3-L1 adipocytes using a novel reporter molecule. J. Biol. Chem. **275:**4787–4795.
41. **Thong, F. S., C. B. Dugani, and A. Klip.** 2005. Turning signals on and off: GLUT4 traffic in the insulin-signaling highway. Physiology (Bethesda) **20:**271–284.
42. **Ugi, S., T. Imamura, H. Maegawa, K. Egawa, T. Yoshizaki, Shi.K., T. Obata, Y. Ebina, A. Kashiwagi, and J. M. Olefsky.** 2004. Protein phosphatase 2A negatively regulates insulin's metabolic signaling pathway by inhibiting Akt (protein kinase B) activity in 3T3-L1 adipocytes. Mol. Cell. Biol. **24:**8778–8789.
43. **Varadi, A., T. Tsuboi, and G. A. Rutter.** 2005. Myosin Va transports dense core secretory vesicles in pancreatic MIN6 beta-cells. Mol. Biol. Cell **16:**2670–2680.
44. **Wang, Q., R. Somwar, P. J. Bilan, Z. Liu, J. Jin, J. R. Woodgett, and A. Klip.** 1999. Protein kinase B/Akt participates in GLUT4 translocation by insulin in L6 myoblasts. Mol. Cell. Biol. **19:**4008–4018.
45. **Wu, X., B. Bowers, K. Rao, Q. Wei, and J. A. Hammer III.** 1998. Visualization of melanosome dynamics within wild-type and dilute melanocytes suggests a paradigm for myosin V function In vivo. J. Cell Biol. **143:**1899–1918.
46. **Wu, X., G. Jung, and J. A. Hammer III.** 2000. Functions of unconventional myosins. Curr. Opin. Cell Biol. **12:**42–51.
47. **Yoshizaki, T., H. Maegawa, K. Egawa, S. Ugi, Y. Nishio, T. Imamura, T. Kobayashi, S. Tamura, J. M. Olefsky, and A. Kashiwagi.** 2004. Protein phosphatase-2C alpha as a positive regulator of insulin sensitivity through direct activation of phosphatidylinositol 3-kinase in 3T3-L1 adipocytes. J. Biol. Chem. **279:**22715–22726.